RECYCLING POLYOLEFIN FILMS VIA FIELD-ASSISTED EXTRUSION

Mansoureh Jamalzadeh, Margaret J. Sobkowicz*, David O. Kazmer, Patrick Casey, University of Massachusetts Lowell Plastics Engineering Department

E. Bryan Coughlin, University of Massachusetts Amherst Polymer Science and Engineering Department

*Margaret_sobkowiczkline@uml.edu, 978-934-3433

Abstract

Flexible polymer films have an increasing share of the single-use packaging market. The recycling rate for these films remains low due to challenges in collecting and handling this film, but also because many films contain multiple layers, and the compositional complexity degrades the quality of secondary feedstocks. Linking innovations in separations, characterization, and product redesign with advanced processing capabilities in the plastics supply chain will be key to scaling circular economy innovations. This work describes state-of-the-art extrusion approaches for recovering value from flexible films and mixed plastic packaging waste streams that are particularly challenging to recycle. The first case study describes the ultrasonication-assisted extrusion of polyethylene to manipulate the crystalline structure in pursuit of improved gas barrier properties without additional polymer layers. A custom-built sonication die is employed for controlling the dynamic temperature and shear environment, resulting in flow-induced crystallization. A second case study investigates compatibilization via gamma irradiation to induce free radical reactions in polymer blends. The residual radical centers induce grafting that alters the blend morphology and properties. The relationships between extrusion processing parameters, polymer structure, and performance are explored using spectroscopy, rheology, and scattering. These case studies show that melt processing is an efficient and adaptable approach for achieving property improvements in mixed waste streams, and for producing films that are more sustainable by design.

Introduction and Motivation

Multilayered plastic films are composed of heterogeneous components that were developed to overcome polyolefin films' high oxygen permeability. Using an external field during the extrusion process rather than specialized polymer formulations or additives is a more universally applicable solution for producing high-performance films that are inherently recyclable. Ultrasonic-assisted crystallization can improve the barrier properties of polyethylene films by accelerating the crystallinity and altering the crystal structure. However, it is crucial to examine the effect of factors such as polymer structure, processing conditions, and ultrasonic power in improving crystallinity. For heterogenous recycled polymer blends, irradiation-induced grafting reactions at the interface of components is a potential method for improving the compatibility of immiscible polymers without addition of designer chemicals. The effects of ionizing radiation on polymers depend on factors such as polymer structure, environmental conditions, and irradiation dose; detailed studies are necessary to optimize their application for specific polymer materials and recycling purposes.

This paper explores the use of ultrasound to modify crystal structure such that it can enhance the oxygen barrier of monolayer polyethylene film during the continuous film extrusion process. We also demonstrate gamma irradiation as a means of inducing interfacial reactions in PET and LLDPE blends, since these polymers are some of the most common materials used in multilayered food packages. The first case emphasizes design for recycling such that multilayer films are no longer necessary, whereas the second case explores compatibilization when multilayer or multicomponent materials end up in the waste stream.

Review of related work

Gases diffuse through the amorphous parts of polymer films because the chains are more flexible than in the crystalline region, with free volume to accommodate the small molecules. The crystal structure formed during the processing of polyethylene film thus has a significant impact on the oxygen permeation rate.[1] This crystal structure develops under complex conditions that involve high cooling rates, variable shear rates, and pressure.[2] Researchers have explored

these factors in various studies related to non-isothermal crystallization, flow-induced crystallization (FIC), and polymer crystallization under pressure. The crystallization kinetics of high-density polyethylene under non-isothermal conditions starts with random nucleation followed by isotropic growth of spherulites.[3] Deformation applied to the semicrystalline polymer melt during the process can significantly enhance the concentration of nuclei and even change the final crystalline morphology to anisotropic structures.[4] Although ultrasound-assisted crystallization was shown to accelerate the nucleation rate and better control the formation and growth of crystals, the limited understanding of how the ultrasonic field interacts with polymer melt restricts its practical application during polymer processing.[5,6] One possible mechanism for the effect of ultrasound is its influence on the vibrational motion of polymer chains, which is intrinsically linked to the material's viscoelastic properties and molecular characteristics.[5] Increasing the ultrasound vibration frequency and amplitude was shown to reduce the viscosity of some polymer melts due to the applied shear stress.[7]

The irradiation-assisted approach enhances the compatibility of immiscible polymer blends by inducing free radical interface reactions between the polymer components.[8] The irradiation-assisted method is particularly interesting because in principle it can be applied in a single-step, continuous process that does not require an additive tailored for every new material system. The effectiveness of the irradiation-assisted method depends on the susceptibility of the polymer chemical structure to free radical attack, the stability of those free radicals, and environmental conditions, such as air or vacuum. In a vacuum, the concentration of free radicals increases, which facilitates interface reactions.[9] Irradiated PET undergoes branching and chain scission, producing free radicals that can react with LLDPE during reactive extrusion compounding.[10]

The objective of the first case study was to discern the effects of applying ultrasound at the extruder die lip, to induce FIC while cooling the polymer thereby manipulating crystallinity and crystal structure. In pursuit of this aim, a home-built sonication die was designed to study the effect of the ultrasonic field during cast film extrusion on polyethylene crystallinity and its final mechanical and physical properties. The second case study explores the compatibility of PET/LLDPE blends using post-irradiated PET pellets containing free radicals, compounded with LLDPE via reactive extrusion in a twin-screw extruder. The effects of free radical interfacial reactions were evaluated by examining the rheological, mechanical, and morphological properties of PET/LLDPE blends. The grafting interface reactions were found to impact these properties by altering interfacial adhesion, which affects stress transfer at the interface.

Technology Approach

Ultrasonic-Assisted Film Extrusion

Material

The experiment was conducted using high-density polyethylene (HDPE) supplied by Braskem America. Its density is 0.955 g/cm³ and the melt flow index is 0.35 g/10 min (at 190 °C with a load of 2.16 Kg).

Cast film Extrusion Processing

The extrusion cast film process was executed using a single screw extruder from Collin Lab & Pilot Solutions, complemented by a take-off unit from Thermo Haake equipped with three driven rollers cooled using a constant temperature circulating bath. The home-built sonicator, designed for this purpose, operates at a frequency of 20 kHz with a maximum amplitude of 8 μm. The temperature profile during the extrusion process was set to exceed the melting temperature of HDPE, reaching a maximum of 180 °C. It then gradually decreased to 145 °C at the die, which is approximately the equilibrium melt temperature of HDPE. The melt flow was cooled under extension on the roll stack at a temperature of 60°C and a linear speed of approximately 300 cm/min, resulting in a draw ratio of 5. This temperature setting, between the equilibrium melt temperature (145 °C) and the endpoint of the crystallization peak (60 °C), was chosen to fall within the range of HDPE crystallization as indicated by the DSC results[11] (Figure 1). Setting the equilibrium melt temperature of HDPE at the die increases the pressure as the melt begins to solidify, but we hypothesize that the ultrasonic shear will also be more efficient in the crystallization process, as it will initiate at this temperature.[12] The processing parameters of cast film extrusion with and without the ultrasonic field applied are presented in Table 1.

Table 1: Processing parameters of cast film extrusion

Sample	Die temperature (°C)	Roller temperature (°C)	Puller speed (cm/min)	Draw ratio	Ultrasonic Level
A	145	60	300	5	0
B					3

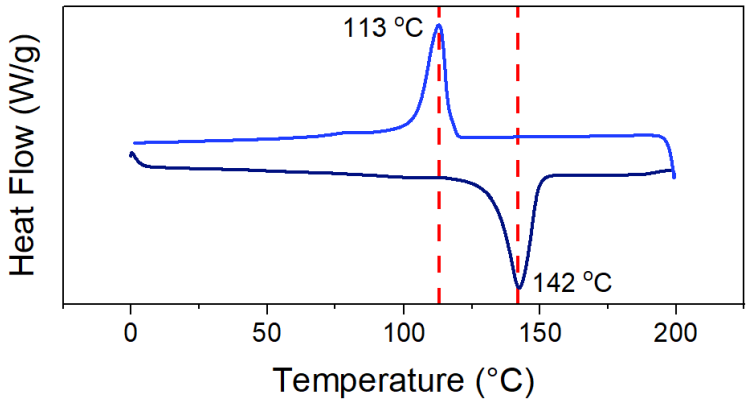

Figure 1: Differential scanning calorimetry showing the thermal transitions of HDPE.

Irradiation-assisted reactive extrusion

Materials

In this experiment, poly(ethylene terephthalate) (PET) was supplied by Indorama Ventures Polymers Germany GmbH. The specific grade used was XPURE 4004, which has an intrinsic viscosity (IV) of 0.64 dl/g. Batches of PET pellets were exposed to gamma irradiation at 2 kGy/hr in the UMass Lowell Radiation Facility gamma cave under vacuum up to 50 and 200 kGy. linear low-density polyethylene (LLDPE) was obtained from Dow Chemical Company. The grade of LLDPE was DOWLEX TM 2552E, which contains no additives and to maximize its susceptibility to free radical interface reactions during compounding. This LLDPE features a high melt flow rate of 25 g/10 min at 190°C and 2.16 kg, with a density of 0.92 g/cm³.

Compounding process

A corotating, intermeshing twin-screw extruder (TSE) with a 15 mm screw diameter and L/D=60:1 from TECHNOVEL Corporation, model KZW15 TW, was used to compound PET/LLDPE. The compounding process was conducted by setting a maximum temperature of 265 °C, a feeding rate of 5 g/min, and screw speed of 100 rpm. Neat/irradiated PET pellets were dried for one hour at 100°C, then mixed with LLDPE at 20% volume fraction PET. Notably, there were no delays between irradiation and compounding.

Characterization

Differential scanning calorimetry (DSC) was conducted using the METTLER TOLEDO model. heat flow enthalpy was measured in a heat-cool-heat cycle with ± 10 °C/min at temperature range of 25 – 200 °C.

The wide-angle X-ray diffraction scattering (WAXS) test was performed using a Rigaku SmartLab WAXS unit equipped with a copper x-ray tube with a wavelength of 0.154 nm. The scattering was measured with a current of 2 mA and a voltage of 20 kV for 10 minutes.

The tensile properties were measured using an Instron model 5966 tensile machine with ASTM D638 at ambient temperature. In ultrasonic-assisted extrusion, samples were cut into dog bone shape (IV) from HDPE film, and the test was done at an extension rate of 10 mm/min. In irradiated-assisted reactive extrusion, samples were prepared using an Xplore microinjection molding machine, and tensile tests were conducted at a crosshead speed of 5 mm/min.

Oxygen transfer rate (OTR) was measured at ambient temperature and 0% humidity with Mocon Ametek OX TRAN 2/22 series following ASTM D3985). Foil masks with a circular area of 1 cm^2 were used to lower the area of permeation on the HDPE films.

The rheological properties were measured by a parallel plate rheometer (ARES-G2) with a 25 mm stainless steel plates from TA Instruments. The disk samples were prepared using a microinjection molding by Xplore Instruments after drying the samples at 120 °C for at least 4 hr. A strain sweep was first performed to determine the linear viscoelastic region, and a 5% strain value was chosen for the frequency sweep tests at 265 °C from 0.1 to 100 rad/s under nitrogen gas. Then, the frequency sweeps rheological data was converted into the stress relaxation modulus G(t) using an analysis routine available in the Trios software.

Discussion

Ultrasonic-Assisted Film Extrusion

Crystallinity

The ultrasonic field's impact on HDPE's crystallinity and crystal structure were analyzed using wide-angle X-ray scattering (WAXS). The crystallinity percent and the degree of orientation after cast film extrusion processing were examined by the WAXS method and presented in Table 2.

Table 2: WAXS data after cast film extrusion

Sample	Peak Intensity (110 plane) cps	Peak Intensity (200 plane) cps	Crystallinity percent (%)	Orientation index	FWHM °	Crystal size (A°)
A	1.29	0.61	52.2	4.6	0.515	164
B	1.53	0.29	59.4	5.2	0.529	159.7

The crystallinity percent is based on the integrated area of the two sharp crystal peaks divided by the total area under the crystal peaks and amorphous halo. The result shows an increase from 53% to 59% after applying the ultrasonic field. The WAXS scattering patterns and the scattering intensity versus the diffraction angle corresponding to the 110 (at 2θ = 21.5º) and 200 (at 2θ = 23.9º) planes at different azimuthal angle segments (β) are shown in Figure 2. When scattering is not uniformly distributed around the 2D WAXS pattern, some degree of crystal orientation is present. The orientation index can be used to quantify the anisotropy, as defined in Equation (1).

$$\text{Orientation index} = I(q)_{@\beta=140\text{-}240} / I(q)_{@\beta=40\text{-}140} \qquad (1)$$

The orientation index shows a slightly higher value after the application of an ultrasonic field, indicating that the crystal planes are more aligned parallel to the film surface.

The crystal size (D) is gained from Scherrer's formula, Equation 2, which shows an inversely proportional relationship with the full-width half maximum (FWHM °) of scattered X-ray expressed in term of $B_{hkl}(2\theta)$. The wavelength of X-rays λ is 1.54 A° for Cu Kα radiation.

$$D = {}^{0.94\,\lambda}/_{B_{hkl}\cos(\theta)} \qquad (2)$$

The result shows a slight reduction in crystal size with the implementation of an ultrasonic field. The higher crystallization percent simultaneously with lower crystal size can be attributed to the creation of more crystal nuclei with sonication.

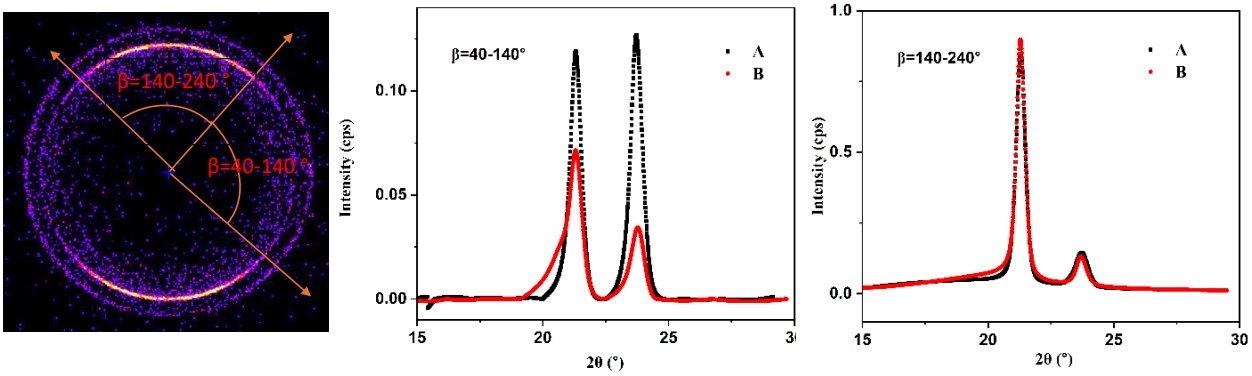

Figure 2: Scattering intensity in different ranges of β and average intensity compared for samples A (without sonication) and B (with sonication).

Mechanical and physical properties

The evolution of crystallinity, influenced by melt flow and the application of an ultrasonic field during polymer processing, significantly impacts the mechanical and physical properties of HDPE, as shown in Table 3. The oxygen transmission rate (OTR) and gas permeation rate through HDPE film decreased after introducing the ultrasonic field. This reduction is due to the formation of a finer and more uniform crystal structure, which makes the diffusion of oxygen gas more challenging. Additionally, the tensile properties demonstrate the ultrasonic field's effect on crystal structure, enhancing toughness under physical load. HDPE exhibits a lower elastic modulus and a higher elongation at break, indicating the formation of smaller crystal sizes after exposure to the ultrasonic field.

Table 3: Mechanical and physical properties data

Sample	Gas Permeation (cc.mil/(m^2.day))	OTR (cc/(m^2.day))	Modulus [MPa]	Tensile strain at Break [%]	Tensile stress at Break [MPa]
A	6516.7	484.5	1468.6	57.5	60.2
B	6463.6	455.2	1351.5	132.7	68.4

Irradiation-assisted compatibilization

Rheology

The rheological behavior of polymer melts can provide valuable insights into the structure and morphology of polymer blends. This research investigates the irradiation-induced interface reaction between the components of polymer blends by examining their rheological properties. As illustrated in Figure 3(a), the storage modulus of PET after irradiation shows a reduction in the high-frequency region, indicating PET degradation. Conversely, there is an increase in the low-frequency region (< 1 rad/s), which signifies that irradiation has induced branch or graft structures in PET.[13] Additionally, the effects of interfacial interactions can be tracked in the blend's elasticity at low-frequency, as immobilization at the interface introduces an additional relaxation mechanism to the neat blend components.[14] Figure 3(b) shows the storage modulus of the PET/LLDPE (20/80%) blend after compounding. The blend of 50 kGy irradiated PET with LLDPE (50 kGy PET/LLDPE (20/80%)) demonstrates a decrease in storage modulus but a longer plateau in comparison to the neat blend. This change can be attributed to irradiation-induced interface reactions, as well as LLDPE degradation due to free radicals' residue of irradiated PET during compounding. This finding aligns with the results of reactive extrusion by Shahbazi et al., which showed interfacial reactions leading to decreased storage modulus by forming PE-g-PS copolymers at the interface.[15] Figures 3(c) and 3(d) show the stress relaxation modulus of the individual blend components (PET before and after irradiation, as well as LLDPE) and the blend after

compounding. The stress relaxation modulus of the blends reflects both the effects of interface grafting reactions and the intrinsic properties of each polymer.[16,17] Polymers exhibit a range of relaxation timescales for stress relaxation moduli. The shortest relaxation time (τ_0) is linked to the monomers, as the Rouse model describes whereas the longest relaxation time (τ_{rep}), known as the reptation time, is affected by the density of entanglements and the overall length of the polymer chain. Additional modes can account for larger structure dynamics such as dispersed droplet deformation and interfacial relaxations in a blend. After irradiation, PET's reptation time increased due to the formation of its branched structure as shown in Figure 3(c). The blend of 50 kGy PET/LLDPE (20/80%) showed an increased reptation time in Figure 3(d), indicating improved interfacial interactions between the blend components. This increase can be attributed to the PET's branched structure and the irradiation-induced interface reactions. However, the blend containing 200 kGy PET (200 kGy PET/LLDPE (20/80%)) exhibited a significant reduction in reptation time. This reduction is because of more degradation of LLDPE which dominates over the irradiation-induced interface reactions in compounding with 200 kGy PET having the higher intensity of free radicals.[13]

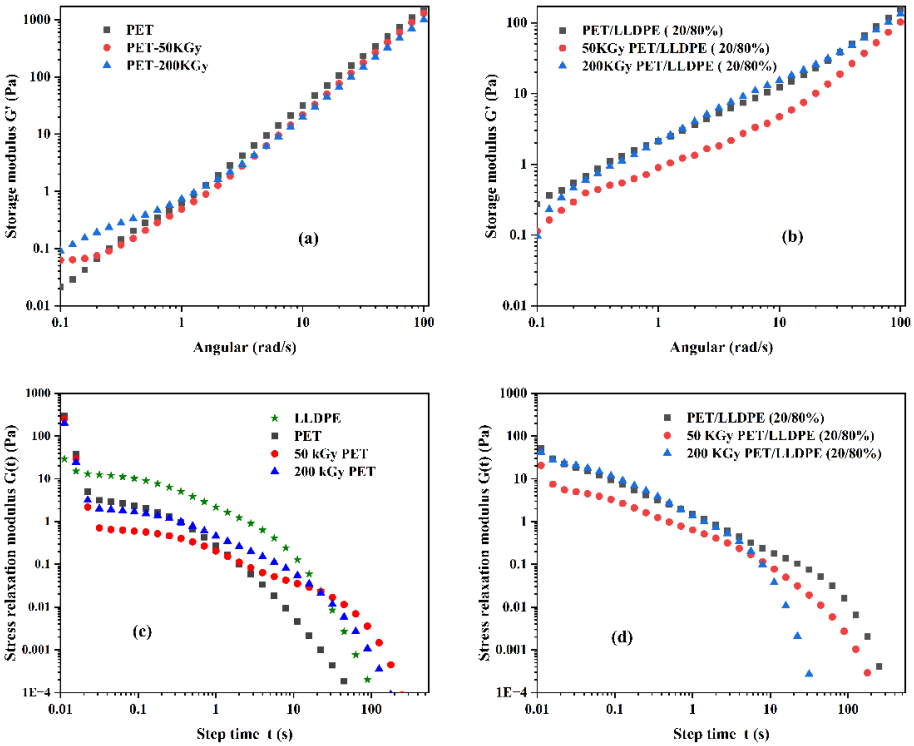

Figure 3: Rheological properties result; (a)&(b) the storage modulus of neat/irradiated PET and its blend with LLDPE (c)&(d) the stress relaxation modulus of blends components individually and after compounding

Morphology

The morphology of immiscible polymer blends has a significant impact on the mechanical properties and performance of the blend. Figure 4 shows the SEM images of PET/LLDPE blends at X1,000 magnification after reactive extrusion, cryofracture, and NaOH treatment to remove the PET phase from the surface. No significant change was observed in the droplet size in the irradiated PET/LLDPE blends, which suggests that interfacial interactions did not prevent coalescence or modify the surface tension, despite the rheological changes described previously. Although other studies on compatibilization show changes in droplet size or even a cocontinuous morphology, the morphology does not reflect the compatibilization here.[18,19] This could be due to changes in the viscosity ratio as the two phases are degraded during processing.[20]

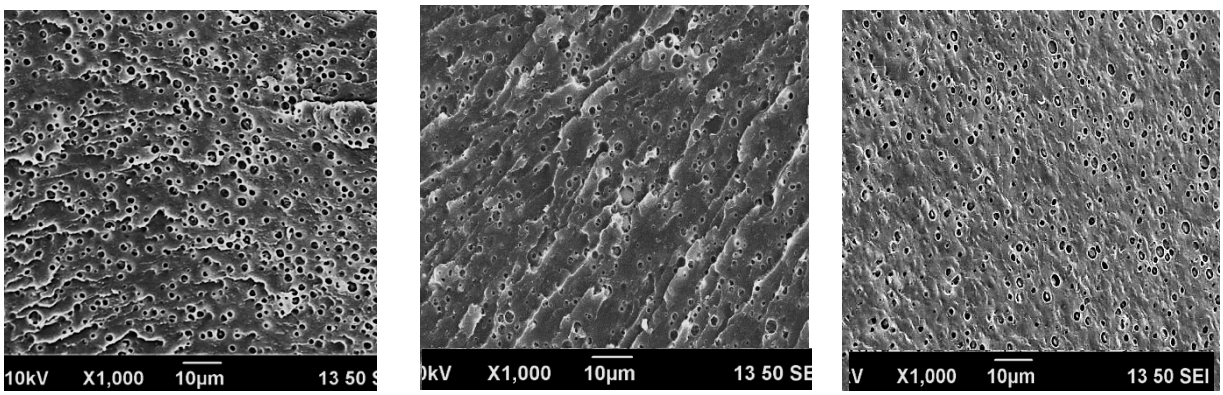

Figure 4: SEM images of PET/LLDPE (20/80%) at different irradiation absorbed doses.

Mechanical Properties

The mechanical properties of pure PET remain nearly unchanged up to an absorbed irradiation dose of 200 kGy, despite the branching and chain scission reactions. However, the mechanical testing of the PET/LLDPE blends shown in Figure 5 demonstrates an improvement in the tensile strength properties after reactive extrusion. The elastic modulus is slightly decreased in 50 & 200 kGy PET/LLDPE (20/80%) but the strain at yield appears to increase. The slight improvement in yield strength of blends shown here can be attributed to interface interaction with irradiated PET, especially at 50 kGy irradiation-absorbed dose. PET/LLDPE blends and composites of PET fiber exposed to irradiation after compounding also showed an increase in yield strength due to intramolecular crosslinking and intermolecular interface reactions.[21] Modification of the extrusion equipment to induce grafting in situ during processing would further enhance the utility of this approach in large scale manufacturing environments.

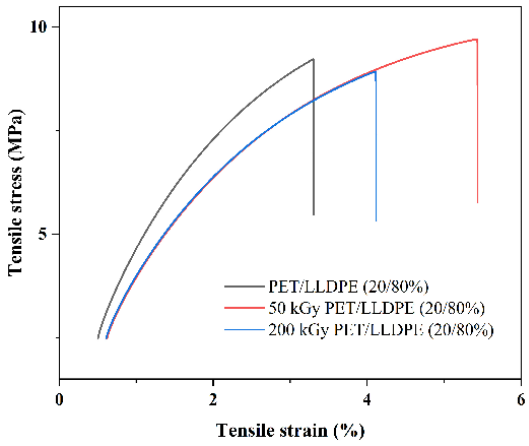

Figure 5: Representative tensile stress-strain curves for PET/ LLDPE (20/80%) after reactive extrusion

Conclusion and Recommendations

The case studies presented here demonstrate multiple approaches to improved recycling of plastic waste via processing innovations. Ultrasonic field assisted extrusion is capable of manipulating polyethylene crystal structure to improve its physical properties without the need for laminating other materials to the film. More work is needed to fully map out the relationships among dynamic temperature and shear, ultrasound power, die geometry, and structure and properties of the film. Radiation-induced compatibilization showed moderate improvement in the dispersion of the

minority phase in PET-LLDPE blends, along with some improvement in mechanical strength. Lack of change observed in the blend morphology indicates that the percent of interchange reactions at the interfaces between the two polymers was low despite the high irradiation dose. Future work should explore more targeted radiation processing perhaps performed in the melt during mixing. The effects of radiation on polymer blends may have additional implications for polymers in the environment (e.g., exposed to UV) or in sterile medical devices. Application of field-assisted processing at multiple points on the supply chain offers many opportunities to improve plastics circularity.

Acknowledgement

This material is based upon work supported by the National Science Foundation under grant #2229091.

References

(1) Todd, W. G. Variables That Affect/Control High-Density Polyethylene Film Oxygen–Moisture Barrier. *J. Plast. Film Sheeting* **2003**, *19* (1), 209–220. https://doi.org/10.1177/8756087903042072.
(2) Cromer, B.M., Coughlin, E.B. and Lesser, A.J. (2019) Polymer Engineering & Science, 60(2), pp. 380–386. doi:10.1002/pen.25293.; Kida, T.; Janchai, K.; Tokumitsu, K.; Yamaguchi, M. Flow-Induced Crystallization Behavior of High-Density Polyethylene Evaluated by Rheo-Raman Spectroscopic System. *Polym. J.* **2023**, *55* (11), 1141–1150. https://doi.org/10.1038/s41428-023-00821-5.
(3) Muhammad Azeem Arshad. Kinetics of Crystallization Mechanisms in High Density Polyethylene and Isotactic Polypropylene. *Polym. Sci. Ser. A* **2021**, *63* (S1), S23–S33. https://doi.org/10.1134/S0965545X22030014.
(4) Hamad, F. G.; Colby, R. H.; Milner, S. T. Transition in Crystal Morphology for Flow-Induced Crystallization of Isotactic Polypropylene. *Macromolecules* **2016**, *49* (15), 5561–5575. https://doi.org/10.1021/acs.macromol.6b00303.
(5) Ávila-Orta, C.; Espinoza-González, C.; Martínez-Colunga, G.; Bueno-Baqués, D.; Maffezzoli, A.; Lionetto, F. An Overview of Progress and Current Challenges in Ultrasonic Treatment of Polymer Melts. *Adv. Polym. Technol.* **2013**, *32* (S1), E582–E602. https://doi.org/10.1002/adv.21303.
(6) Zhang, Z.; Sun, D.-W.; Zhu, Z.; Cheng, L. Enhancement of Crystallization Processes by Power Ultrasound: Current State-of-the-Art and Research Advances. *Compr. Rev. Food Sci. Food Saf.* **2015**, *14* (4), 303–316. https://doi.org/10.1111/1541-4337.12132.
(7) Ibar, J. P. Control of Polymer Properties by Melt Vibration Technology: A Review. *Polym. Eng. Sci.* **1998**, *38* (1), 1–20. https://doi.org/10.1002/pen.10161.
(8) Clarke, R. W.; Sandmeier, T.; Franklin, K. A.; Reich, D.; Zhang, X.; Vengallur, N.; Patra, T. K.; Tannenbaum, R. J.; Adhikari, S.; Kumar, S. K.; Rovis, T.; Chen, E. Y.-X. Dynamic Crosslinking Compatibilizes Immiscible Mixed Plastics. *Nature* **2023**, *616* (7958), 731–739. https://doi.org/10.1038/s41586-023-05858-3.
(9) Jamalzadeh, M.; Sobkowicz, M. J. Reactive Extrusion of Post-Irradiated Poly(Ethylene Terephthalate) to Improve the Interfacial Interactions in Compounding with Its Immiscible Polyethylene Blends. *Polym. Eng. Sci.* **2024**, *64* (4), 1796–1811. https://doi.org/10.1002/pen.26659.
(10) Jamalzadeh, M.; Sobkowicz, M. J. Review of the Effects of Irradiation Treatments on Poly(Ethylene Terephthalate). *Polym. Degrad. Stab.* **2022**, *206*, 110191. https://doi.org/10.1016/j.polymdegradstab.2022.110191.
(11) Derakhshandeh, M.; Hatzikiriakos, S. Flow-Induced Crystallization of High-Density Polyethylene: The Effects of Shear and Uniaxial Extension. *Rheol. Acta* **2011**, *51*. https://doi.org/10.1007/s00397-011-0605-7.
(12) Hamad, F. G.; Colby, R. H.; Milner, S. T. Onset of Flow-Induced Crystallization Kinetics of Highly Isotactic Polypropylene. *Macromolecules* **2015**, *48* (11), 3725–3738. https://doi.org/10.1021/acs.macromol.5b00386.
(13) Jamalzadeh, M.; Ngendahimana, T.; Sobkowicz, M. J. Correlating Color with Free Radical Concentration in Irradiated Poly(Ethylene Terephthalate). *Polymer* **2024**, 127656. https://doi.org/10.1016/j.polymer.2024.127656.
(14) Raval, H.; Devi, S.; Singh, Y. P.; Mehta, M. H. Relationship between Morphology and Properties of Polyamide-6 Low-Density Polyethylene Blends: Effect of the Addition of Functionalized Low-Density Polyethylene. *Polymer* **1991**, *32* (3), 493–500. https://doi.org/10.1016/0032-3861(91)90455-R.
(15) Shahbazi, Kh.; Razavi Aghjeh, M. K.; Abbasi, F.; Partovi Meran, M.; Mehrabi Mazidi, M. Rheology, Morphology and Tensile Properties of Reactive Compatibilized Polyethylene/Polystyrene Blends via Friedel–Crafts Alkylation Reaction. *Polym. Bull.* **2012**, *69* (2), 241–259. https://doi.org/10.1007/s00289-012-0751-9.

(16) Dealy, J. M.; Read, D. J.; Larson, R. G. 4 - Linear Viscoelasticity—Fundamentals. In *Structure and Rheology of Molten Polymers (Second Edition)*; Dealy, J. M., Read, D. J., Larson, R. G., Eds.; Hanser, 2018; pp 105–145. https://doi.org/10.3139/9781569906125.004.
(17) Al-Itry, R.; Lamnawar, K.; Maazouz, A. Rheological, Morphological, and Interfacial Properties of Compatibilized PLA/PBAT Blends. *Rheol. Acta* **2014**, *53* (7), 501–517. https://doi.org/10.1007/s00397-014-0774-2.
(18) Jiang, W.-R.; Bao, R.-Y.; Yang, W.; Liu, Z.-Y.; Xie, B.-H.; Yang, M.-B. Morphology, Interfacial and Mechanical Properties of Polylactide/Poly(Ethylene Terephthalate Glycol) Blends Compatibilized by Polylactide-g-Maleic Anhydride. *Mater. Des.* **2014**, *59*, 524–531. https://doi.org/10.1016/j.matdes.2014.03.016.
(19) Abdel Tawab, K.; Ibrahim, S. M.; Magida, M. M. The Effect of Gamma Irradiation on Mechanical, and Thermal Properties of Recycling Polyethylene Terephthalate and Low Density Polyethylene (R-PET/LDPE) Blend Compatibilized by Ethylene Vinyl Acetate (EVA). *J. Radioanal. Nucl. Chem.* **2013**, *295* (2), 1313–1319. https://doi.org/10.1007/s10967-012-2163-6.
(20) Rao, B. S.; Sridhar, V.; Indira, S.; Punnaiah, G.; Venkatapparao, T. Temperature and Dose Dependency of Free Radicals in Irradiated Poly(Ethylene Terephthalate). *Radiat. Eff. Defects Solids* **2006**, *161* (1), 31–39. https://doi.org/10.1080/10420150500493170.
(21) Meri, R. M.; Jablonskis, I.; Zicans, J.; Kalnins, M.; Bledzki, A. K. DEFORMATIONAL PROPERTIES OF IRRADIATED COMPOSITE MATERIALS BASED ON PET AND PE. *Mech. Compos. Mater.* **2004**, *40* (3), 383–392. https://doi.org/10.1023/B:MOCM.0000033267.84630.4b.
(22) Satapathy, S.; Nag, A.; Nando, G. B. Effect of Electron Beam Irradiation on the Mechanical, Thermal and Dynamic Mechanical Behaviour of Waste Polyethylene-Short PET Fibre Composites. *Polym. Polym. Compos.* **2012**, *20* (7), 647–658. https://doi.org/10.1177/096739111202000709.